

Paleodepositional conditions in the Orca Basin as inferred from organic matter and trace metal contents

Nicolas Tribovillard ^{a,*}, Viviane Bout-Roumazelles ^a, Thomas Algeo ^b, Timothy W. Lyons ^c, Thomas Sionneau ^a, Jean Carlos Montero-Serrano ^a, Armelle Riboulleau ^a, François Baudin ^d

^a Université Lille 1, Laboratoire Géosystèmes, UMR 8157 CNRS, bâtiment SN5, 59655 Villeneuve d'Ascq cedex, France

^b Department of Geology, University of Cincinnati, Cincinnati, Ohio 45221-0013, USA

^c Department of Earth Sciences, University of California, Riverside, CA 92521-0423, USA

^d Université Pierre & Marie Curie – Paris 6, UMR CNRS 7072 Tectonique, Département de Géologie Sédimentaire, 4 place Jussieu, 75252 Paris cedex 05, France

ARTICLE INFO

Article history:

Received 4 October 2007

Received in revised form 21 April 2008

Accepted 28 April 2008

Keywords:

Gulf of Mexico

Holocene

anoxia

euxinia

geochemistry

molybdenum

nickel

chromium

brines

ABSTRACT

The Orca Basin, located in the Gulf of Mexico, is a highly stratified basin that collects sedimentary particles of clastic origin (supplied by the Mississippi River) and of biogenic origin (marine surface productivity). The strong pycnocline induces anoxic bottom conditions that are expected to be favorable to organic matter (OM) accumulation and prone to enrichment of sediments in redox-sensitive trace metals. Here we report on OM and trace metal contents in the upper 750 cm below sea floor (cmbsf) of Core MD02-2552 (mostly Holocene) and deposited under permanently stratified bottom conditions. The organic content is dominated by marine-derived amorphous OM. Contrary to expectations, sedimentary OM in the basin is highly degraded, probably due to a long residence time of organic particles at the basin's basin's halocline at ~2240 m. Also unexpected is the limited sedimentary enrichment of redox-sensitive trace metals. We suggest that the non-enrichment in U and V could be explained by the so-called basin reservoir effect, that is, limited metal availability because of low rates of water renewal in a strongly restricted subpycnocline water mass. The non-enrichment in Cu could have the same cause, plus the fact that the relatively degraded OM may not readily form organometallic complexes. However a marked enrichment is observed for Mo, and a moderate one for Ni and Cr, which could be accounted for by sporadic presence of H₂S in bottom waters. Such occurrences of H₂S would not be sufficient to promote a detectable FeS to FeS₂ conversion, but they would induce the capture of Mo in the form of thiomolybdate and accessorially Ni–Cr as Ni–CrO₄ complexes.

© 2008 Elsevier B.V. All rights reserved.

1. Introduction

Within the Gulf of Mexico, the Orca Basin is exceptional in that rapid sedimentation (about 1 m/kyr) sustained by high rates of terrigenous clastic input and marine productivity make the basin an excellent recorder of past environmental conditions of sediment deposition (Sheu and Presley, 1986; Sheu, 1990; Van Cappellen et al., 1998; Hurtgen et al., 1999). Its stratified water mass induces anoxic bottom conditions that are potentially favorable to organic-matter preservation and accumulation of redox-sensitive trace metals.

In this paper we report on the quantity and sources of organic matter (OM) in Orca Basin sediments of recent, mostly Holocene age, as well as their trace metal contents (redox-sensitive, productivity-related and/or sulfide-forming elements), with an eye toward depositional conditions that have prevailed in the Orca Basin since the development of strongly stratified conditions at least 8000 yr ago. In the present study, we

explore the trace metal contents of the Orca sediments, for which few published data are available.

2. The Orca Basin, description and previous work

The Orca Basin is an intraslope depression in the northern Gulf of Mexico (Fig. 1) characterized by strong water-column stratification (Fig. 2; Sheu, 1990; Van Cappellen et al., 1998; Hurtgen et al., 1999). The origin of the depression is related to regional salt tectonics along the Louisiana continental slope (Trabant and Presley, 1978). Morphologically, the basin is a 400-km² elbow-shaped depression with water depths ranging from about 1800 to 2400 m in the deepest portions (Fig. 1). There are two sub-basins separated by a medial saddle. The Orca Basin has a highly stable, anoxic brine pool, and the bottom 200 m of the Orca Basin, including the saddle, are permanently anoxic (Sheu and Presley, 1986; Van Cappellen et al., 1998; Hurtgen et al., 1999; Lyons and Severmann, 2006) and maintain a salinity of >260 g/l due to the dissolution of shallow subsurface salt diapirs (Shokes et al., 1977; Sheu et al., 1987). Geochemical analysis of major components in the Orca Basin brine fingerprint its source to dissolution of the regionally

* Corresponding author.

E-mail address: Nicolas.Tribovillard@univ-lille1.fr (N. Tribovillard).

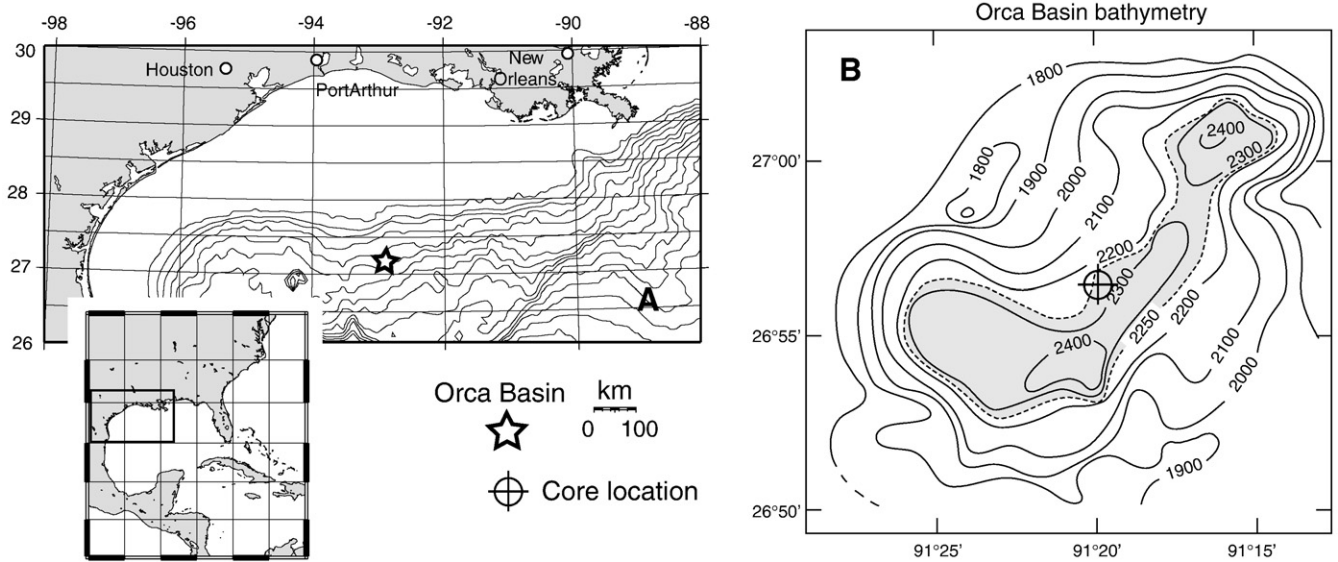


Fig. 1. Location (A) and bathymetry (B) of the Orca Basin in the Gulf of Mexico. The general maps were drawn using the online map creation device at the following website: <http://www.aquarius.ifm-geomar.de/>. The bathymetry map is redrawn from Shokes et al. (1977). Contours in meters. The shaded area shows the portion of the basin filled with brines.

pervasive, halite-rich Jurassic Louann Salt deposit (Sheu, 1990). Down-core decreases in pore-water salinity point to lateral inputs, perhaps via a ‘brine river’ (Brooks et al., 1990), rather than sourcing from beneath the basin. This conclusion is supported by evidence for seafloor exposures of salt north and southeast of the basin (Addy and Behrens, 1980). The brine pool has an estimated total volume of 5 km^3 (Schijf, 2007). The seawater overlying the basinal brine has a typical marine salinity of 35 g/l. The resulting density contrast at the seawater–brine interface between the depths of 2200 and 2250 m induces a strong stratification of the water column. Oxygen depletion results from organic-matter decomposition and restricted oxygen renewal across the stable brine–seawater interface. A large fraction of the particulate matter settling into the basin is trapped at the salinity transition region (2200–2250 m; Sheu, 1990; Schijf, 2007); and the trapped particulates contain up to 60% organic matter (Trefry et al., 1984; Van Cappellen et al., 1998). Wong et al. (1985) and Sheu (1990) noted that the settling organic matter is trapped at the stable brine–sea water interface long enough to undergo a notable degradation. This degradation is reflected by the marked release of biogenic iodine at the pycnocline.

Addy and Behrens (1980) estimated the beginning of brine inputs at ca. 8000 years BP based on radiocarbon dating of an abrupt up-core transition from gray, presumably oxic sediment to black mud. However, a salinity study of the interstitial water from a DSDP core (site 618, Leg 96) led Presley and Stearns (1986) to propose that anoxia could have existed in the basin for at least 50,000 yr.

H_2S in the Orca water column is present in low concentrations in response to bacterial sulfate reduction but noticeable amount of dissolved H_2S are restricted to the region just below the brine–seawater interface (Sheu, 1990; Schijf, 2007; Fig. 2). Dissolved sulfate and reactive iron are abundant at all depths and do not limit iron sulfide production (Sheu and Presley, 1986). The near absence of H_2S deeper in the water column has been attributed to low rates of sulfate reduction as well as its rapid reaction with reactive Fe to form FeS (Sheu, 1990; Van Cappellen et al., 1998; Hurtgen et al., 1999). Evidence for syngenetic iron sulfide formation has been documented in the lower portion of the transition zone of the water column (Trefry et al., 1984; Van Cappellen et al., 1998; Hurtgen et al., 1999). The reactive Fe necessary for FeS formation is scavenged by dissolved H_2S (or HS^-) in the lower portion of the redox transition zone. H_2S was below detection ($3 \mu\text{M}$) within the upper basinal sediments, suggesting effective consumption by Fe in combination with low rates of in situ production (Hurtgen et al., 1999) The excess

of reactive Fe relative to the production of H_2S has significant implications for the amount of pyrite formed via mechanisms involving both H_2S and intermediate S species. As explained by Hurtgen et al. (1999), one can observe an appreciable depth difference between the location of sulfide oxidation and concomitant production of intermediate S species in the upper transition zone and the production of FeS deeper in the transition zone. In addition, the very low abundance of free H_2S in the sediment hampers the transformation of FeS to FeS_2 . This

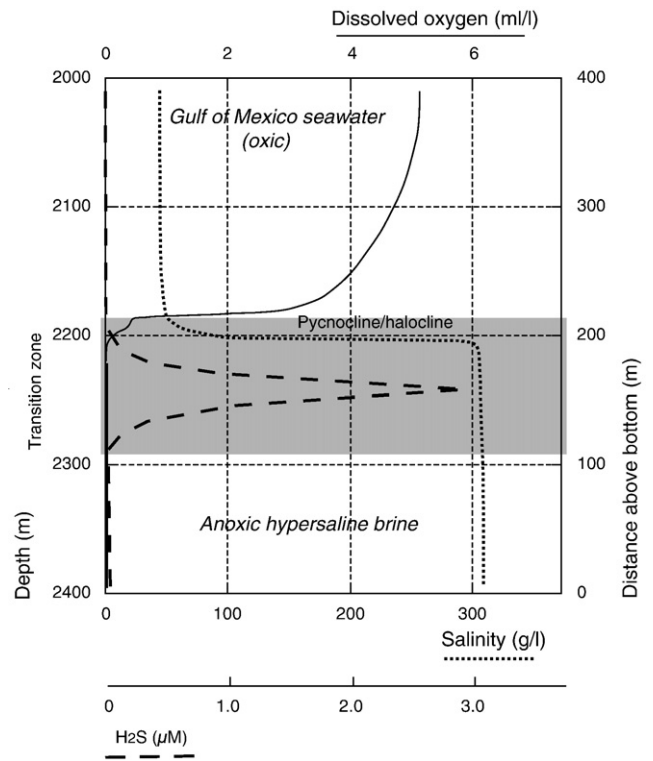


Fig. 2. Depth profiles of dissolved oxygen, dissolved H_2S and conductive salinity in the Orca Basin (redrawn from Sheu and Presley, 1986; Schijf, 2007). Shaded: transition zone between normal sea water and the restricted bottom waters.

situation causes pyrite to be undetectable in the sediment (except for grey-colored, non-laminated, layers where detectable FeS to FeS₂ conversion could occur and form pyrite; Sheu and Presley, 1986; Sheu, 1990; but note that such grey levels are not observed in the core studied here that is entirely laminated), although concentrations of S as HCl-soluble “FeS” range up to 1.86 wt.% (Hurtgen et al., 1999). Lastly, Sheu and Presley (1986) and Sheu (1990) observed no evidence for marked enrichment in trace metals (U, Cu, Ni, Zn, Pb and Cd) in the Orca Basin sediment, nor in the brines at the base of the water column.

3. Materials and methods

3.1. Sampling

We sampled core MD02-2552 collected during the 2002 cruise of the R/V *Marion-Dufresne* (IMAGES or International Marine Global Change Study, and PAGE or Paléocéanographie de l'Atlantique et Géochimie programs). The core location is: latitude 26°56.80 N, longitude 91°20.72 W, water depth 2240 m. The corer was the Calypso II type. The sediments consist entirely of black microlaminated (mm- to cm-scale) mud (silty clay). Fronds of unaltered *Sargassum* are ubiquitous

throughout the sampled sediments. Sediment samples were taken every 10 cm through the upper 7.5 m of the core, yielding a total of 75 samples.

3.2. Methods

For all samples, carbonate content was measured using a Bernard calcimeter (which measures the amount of released CO₂ following acid digestion). Grain size determination was carried out on the carbonate-free fraction of the sediment using a Malvern Mastersizer 2000 apparatus. Two parameters are reported here: sorting and median grain size. Rock Eval pyrolysis parameters were determined with a Delsi Oil Show Analyser (Rock Eval II): total organic carbon content (TOC, in wt wt.%), Tmax (°C), and Hydrogen Index (HI, in mg hydrocarbon per g TOC; see Espitalié et al., 1986, and Espitalié, 1993, for procedural details). The Tmax index is the temperature that is recorded for the peak of hydrocarbon release during artificial maturation through pyrolysis. Tmax is thus a proxy for the maturation of OM. Standard palynological processing techniques, as described in Lallier-Vergès et al. (1997) were used to prepare total untreated kerogen slides from the residues of HCl and HF digestion. The mounting medium of the slides was Elvacite 2044. The nature of the

Table 1
Trace metal data for the bulk sediment and for the clay-sized fraction

| Bulk sediment | | | | | | | | | | | | |
|--------------------|----------------------------|---------------------------|----------------------------|----------------------------|----------------------------|----------------------------|----------------------------|----------------------------|----------------------------|---------------------------|----------------------------|-----------------|
| Depth (cmbsf) | Ba/Al × 10 ⁴ | V/Al × 10 ⁴ | Cr/Al × 10 ⁴ | Co/Al × 10 ⁴ | Ni/Al × 10 ⁴ | Cu/Al × 10 ⁴ | Zn/Al × 10 ⁴ | Zr/Al × 10 ⁴ | Mo/Al × 10 ⁴ | U/Al × 10 ⁴ | Th/Al × 10 ⁴ | Al (wt wt.%) |
| 40 | 76.9 | 16.9 | 62.3 | 1.3 | 34.8 | 4.4 | 8.8 | 21.8 | 7.6 | 0.3 | 1.4 | 6.44 |
| 130 | 75.2 | 15.7 | 54.6 | 1.2 | 33.0 | 3.7 | 8.9 | 20.7 | 6.7 | 0.3 | 1.4 | 6.37 |
| 200 | 81.1 | 15.0 | 42.4 | 1.2 | 23.5 | 3.9 | 8.9 | 21.4 | 5.2 | 0.3 | 1.4 | 6.29 |
| 230 | 78.5 | 14.9 | 39.1 | 1.1 | 22.5 | 3.4 | 8.3 | 21.9 | 4.8 | 0.3 | 1.4 | 6.42 |
| 280 | 77.2 | 14.2 | 42.1 | 1.1 | 25.5 | 3.0 | 8.5 | 20.8 | 5.0 | 0.3 | 1.4 | 6.61 |
| 300 | 81.9 | 15.2 | 46.6 | 1.2 | 26.7 | 3.4 | 11.4 | 21.8 | 4.9 | 0.3 | 1.4 | 6.33 |
| 340 | 76.6 | 16.0 | 33.8 | 1.8 | 18.0 | 5.3 | 8.6 | 20.0 | 6.3 | 0.3 | 1.5 | 6.45 |
| 380 | 78.0 | 14.6 | 33.1 | 1.0 | 16.9 | 3.3 | 8.1 | 18.9 | 3.8 | 0.3 | 1.4 | 6.88 |
| 490 | 73.7 | 14.9 | 32.2 | 1.1 | 18.4 | 3.8 | 8.8 | 18.9 | 3.7 | 0.3 | 1.4 | 7.02 |
| 681 | 66.1 | 14.1 | 22.2 | 1.1 | 11.7 | 3.1 | 8.7 | 20.3 | 2.1 | 0.3 | 1.4 | 7.27 |
| | Ba EF | V EF | Cr EF | Co EF | Ni EF | Cu EF | Zn EF | Zr EF | Mo EF | U EF | Th EF | |
| 40 | 1.1 | 1.1 | 5.7 | 0.6 | 4.4 | 1.0 | 0.7 | 1.0 | 50.9 | 1.0 | 1.0 | |
| 130 | 1.0 | 1.0 | 5.0 | 0.6 | 4.1 | 0.8 | 0.7 | 0.9 | 44.8 | 1.0 | 1.1 | |
| 200 | 1.1 | 1.0 | 3.9 | 0.6 | 2.9 | 0.9 | 0.7 | 1.0 | 34.6 | 1.0 | 1.1 | |
| 230 | 1.1 | 1.0 | 3.6 | 0.5 | 2.8 | 0.8 | 0.6 | 1.0 | 32.1 | 1.0 | 1.1 | |
| 280 | 1.1 | 0.9 | 3.8 | 0.5 | 3.2 | 0.7 | 0.7 | 0.9 | 33.5 | 1.0 | 1.1 | |
| 300 | 1.1 | 1.0 | 4.2 | 0.6 | 3.3 | 0.8 | 0.9 | 1.0 | 32.6 | 1.0 | 1.1 | |
| 340 | 1.0 | 1.1 | 3.1 | 0.9 | 2.3 | 1.2 | 0.7 | 0.9 | 42.0 | 1.0 | 1.1 | |
| 380 | 1.1 | 1.0 | 3.0 | 0.5 | 2.1 | 0.7 | 0.6 | 0.9 | 25.5 | 1.1 | 1.1 | |
| 490 | 1.0 | 1.0 | 2.9 | 0.5 | 2.3 | 0.9 | 0.7 | 0.9 | 24.9 | 1.1 | 1.1 | |
| 681 | 0.9 | 0.9 | 2.0 | 0.5 | 1.5 | 0.7 | 0.7 | 0.9 | 14.1 | 1.1 | 1.0 | |
| Clay-size fraction | | | | | | | | | | | | |
| Depth (cmbsf) | Ba/Al × 10 ⁴ | V/Al × 10 ⁴ | Cr/Al × 10 ⁴ | Co/Al × 10 ⁴ | Ni/Al × 10 ⁴ | Cu/Al × 10 ⁴ | Zn/Al × 10 ⁴ | Zr/Al × 10 ⁴ | Mo/Al × 10 ⁴ | U/Al × 10 ⁴ | Th/Al × 10 ⁴ | Al (wt.%) |
| 40 | 44.17 | 19.98 | 12.87 | 1.11 | 5.69 | 5.96 | 14.42 | 14.27 | 0.93 | 0.24 | 1.40 | 9.41 |
| 130 | 41.98 | 18.87 | 12.03 | 0.97 | 5.04 | 5.44 | 13.24 | 13.47 | 0.47 | 0.23 | 1.43 | 9.41 |
| 200 | 42.52 | 18.39 | 11.53 | 1.05 | 5.03 | 5.54 | 12.58 | 13.29 | 0.57 | 0.24 | 1.42 | 9.48 |
| 230 | 44.06 | 18.61 | 12.05 | 1.00 | 4.51 | 4.60 | 11.85 | 13.46 | 0.44 | 0.24 | 1.44 | 9.67 |
| 280 | 44.12 | 18.03 | 11.85 | 1.02 | 4.78 | 4.34 | 12.28 | 13.69 | 0.42 | 0.24 | 1.52 | 9.74 |
| 300 | 42.60 | 18.82 | 11.94 | 1.00 | 4.72 | 4.79 | 14.33 | 13.07 | 0.79 | 0.24 | 1.38 | 9.65 |
| 340 | 41.91 | 19.23 | 12.43 | 1.26 | 5.47 | 5.06 | 12.41 | 13.97 | 0.37 | 0.25 | 1.42 | 9.98 |
| 380 | 41.80 | 19.08 | 11.08 | 0.95 | 4.23 | 4.08 | 11.02 | 13.47 | 0.43 | 0.25 | 1.39 | 10.07 |
| 490 | 43.31 | 17.93 | 10.83 | 0.90 | 3.82 | 4.19 | 11.04 | 13.80 | 0.80 | 0.26 | 1.40 | 9.92 |
| 681 | 39.02 | 17.69 | 10.85 | 1.28 | 4.68 | 4.10 | 11.29 | 13.68 | 0.23 | 0.25 | 1.45 | 10.11 |

Enrichment factors (EF) and Al-normalized abundances.

Aluminum content is expressed in weight percent (wt.%). As the trace metals (TM) are expressed in ppm or µg/g, the TM/Al ratios are multiplied by 10⁴. Enrichment factors are calculated as follows:

$EF_{TM} = TM/Al_{sample} : TM/Al_{average\ shale}$. When $EF_{TM} > 1$, the trace metal (TM) of interest is enriched relative to average shale.

palynofacies assemblages was determined by making 300 counts per slide. To estimate the level of preservation of the organic matter the qualitative six-point fluorescence scale of Tyson (1995) was used, based on a global evaluation under blue light fluorescence.

Major- and trace-element analyses were carried out by ICP-AES and ICP-MS, respectively, at the spectrochemical laboratory of the Centre de Recherches en Pétrographie et Géochimie of Vandœuvre-les-Nancy (geochemistry facility of the French Centre National de la Recherche Scientifique). Prior to analysis, the samples were rinsed five times to remove salt. The samples were then prepared by fusion with LiBO₂ followed by HNO₃ dissolution. The analytical accuracy and precision were found to be better than 1% (mean 0.5%) for major and minor elements, 5% for Cr, Mo, U, V and Zn, and 10% for Ni and Cu, as checked by international standards and analysis of replicate samples (Carignan et al., 2001). We determined the chemical composition of the bulk sediment and the clay-size fraction (<2 μm; Table 1). The clay fraction was isolated using the standard protocol for clay–mineral assemblage determination. The acid treatment used to remove calcium carbonate also removes the adsorbed elements from the clay minerals. Consequently, the chemical analysis of this fraction corresponds to the composition of the chemically non-reactive and OM-lean, clay-size, terrigenous supply (Innocent et al., 1999).

The Orca Basin is mainly supplied with land land-derived particles by the Mississippi River (and accessorially the Atchafalaya River). The Mississippi River drains almost half of the conterminous United States (Davies and Moore, 1970; Flocks and Swarzenski, 2007), and as a consequence of this huge catchment, the composition of the detrital flux delivered to the Gulf of Mexico is very close to that of average shale (Flocks and Swarzenski, 2007; Swarzenski et al., 2008). Consequently, we normalized our results to average shale.

3.3. Age model

To date, no accurate age model is available for the upper 750 cm of the core. Only one age datum is available for the studied interval: the sample at 540 cm below sea floor (cmbsf) is dated by ¹⁴C at 9838 yr cal BP. The next ¹⁴C age datum downcore is at 790 cmbsf and is 13,500 yr cal BP. If we extrapolate an age for the base of the sampled interval, the deepest sample would be dated of 12,700 yr cal BP. In view of these age data, the onset of bottom-water anoxia ca. 8000 yr ago proposed by Addy and Behrens (1980) predicts that our sample at 681 cmbsf would have been deposited prior to the development of permanently anoxic conditions. However, Presley and Stearns (1986) argued for an

onset of anoxia about 50,000 yr ago, in which case even our deepest sample would have been deposited under anoxic conditions.

4. Results

4.1. Analytical results

4.1.1. Palynofacies

The palynofacies are dominated by a brown-colored structureless OM, usually referred to as amorphous OM (or AOM; e.g., Tyson 1995). This brown AOM has a heterogeneous “floc” internal structure and “fuzzy” outlines, and it shows a relatively granular texture and hardly-detectable fluorescence. This type of AOM is very common in marine sediments and sedimentary rocks with high OM enrichment (e.g., Gorin and Steffen, 1991; Tribouillard and Gorin, 1991; Lallier-Vergès et al., 1993a, 1993b; Tyson, 1995; Baudin et al., 1999; Tyson and Follows, 2000). It is of marine origin, deriving from bacterial, algal and planktonic sources (Tyson, 1995; Roncaglia and Kujper, 2006; Sebag et al., 2006). Figured (i.e., identifiable) organic elements are also observed: land-derived phytoclasts and marine algae.

4.1.2. Rock Eval parameters

The vertical distributions of the values of the three indices TOC, HI, Tmax are illustrated in Fig. 3 (see also Table 2). A slight increase is observed for TOC and HI from the base of the section to ca. 100–200 cmbsf, followed by a decrease toward the top. Tmax values show a smooth distribution with a very slight decrease upward. A Tmax vs. HI cross plot (Fig. 4) indicates that the studied core contains an immature mixture of type-II and -III OM, i.e., of marine and terrestrial OM, respectively (Espitalié et al., 1986). Fig. 4A shows a rough positive relationship between TOC and HI, and indicates that the four samples that are the richest in OM (TOC>1%) do not yield high HI values. Conversely, a negative correlation is suggested in a Tmax vs. HI crossplot (Fig. 4B) in which the highest Tmax values are associated with the lowest HI value. No relationship can be observed between Rock Eval parameters and the palynofacies constituents.

4.1.3. Grain size distribution

Vertical changes in the grain size of the carbonate-free fraction of the sediment are illustrated in Fig. 3. Both the median and sorting parameters show a steady and rather constant distribution from the base of the section to 380 cmbsf. A transition toward lower values of

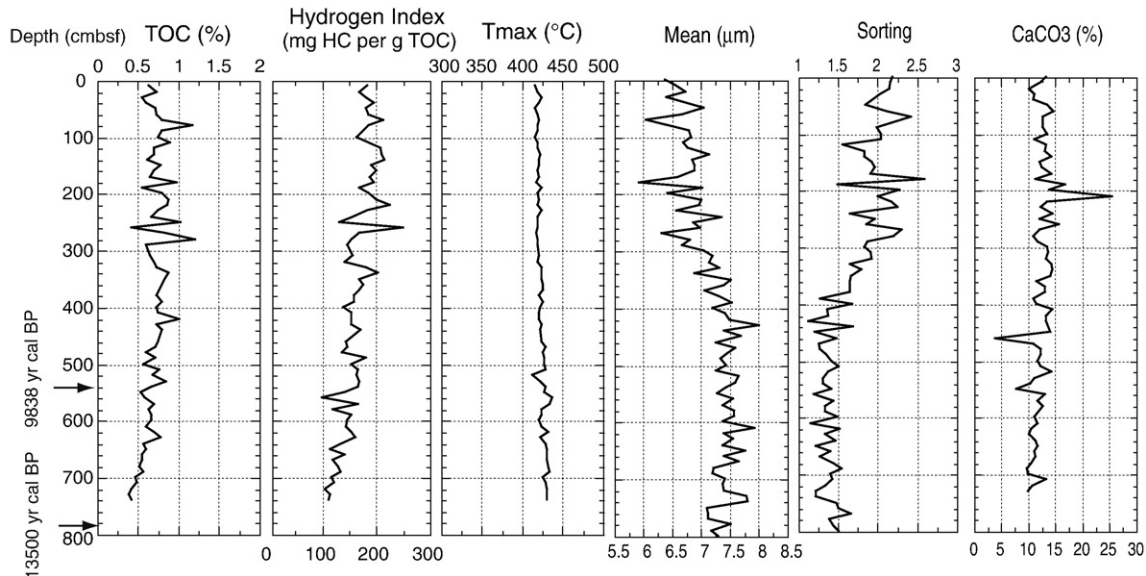


Fig. 3. Stratigraphic distribution of the Rock Eval pyrolysis parameters (total organic carbon or TOC; Hydrogen Index; Tmax), of two grain size parameters (mean and sorting) and of the carbonate content (CaCO₃). ¹⁴C cal BP ages from Sionneau et al. (submitted for publication).

Table 2
Rock Eval pyrolysis parameters

| Depth (cmbsf) | TOC (wt.%) | HI (mg HC/g TOC) | Tmax (°C) | Depth (cmbsf) | TOC (wt.%) | HI (mg HC/g TOC) | Tmax (°C) |
|------------------|---------------|------------------------|--------------|------------------|---------------|------------------------|--------------|
| 10 | 0.64 | 184 | 416 | 380 | 0.74 | 160 | 422 |
| 20 | 0.74 | 170 | 419 | 390 | 0.81 | 161 | 426 |
| 30 | 0.56 | 183 | 424 | 400 | 0.74 | 141 | 423 |
| 40 | 0.61 | 198 | 421 | 410 | 0.76 | 155 | 422 |
| 50 | 0.72 | 183 | 417 | 420 | 1.02 | 154 | 422 |
| 60 | 0.74 | 186 | 420 | 430 | 0.74 | 156 | 425 |
| 70 | 0.81 | 214 | 421 | 440 | 0.81 | 172 | 423 |
| 80 | 1.18 | 188 | 419 | 450 | 0.81 | 172 | 423 |
| 90 | 0.80 | 177 | 420 | 460 | 0.75 | 146 | 424 |
| 100 | 0.75 | 165 | 417 | 470 | 0.72 | 147 | 429 |
| 110 | 0.90 | 186 | 420 | 480 | 0.61 | 137 | 426 |
| 120 | 0.70 | 210 | 420 | 490 | 0.73 | 183 | 428 |
| 130 | 0.71 | 212 | 423 | 500 | 0.58 | 156 | 428 |
| 140 | 0.62 | 216 | 421 | 510 | 0.77 | 168 | 429 |
| 150 | 0.78 | 192 | 421 | 520 | 0.69 | 166 | 413 |
| 160 | 0.70 | 202 | 420 | 530 | 0.86 | 170 | 423 |
| 170 | 0.66 | 189 | 422 | 540 | 0.67 | 167 | 429 |
| 180 | 0.98 | 197 | 418 | 550 | 0.54 | 142 | 428 |
| 190 | 0.56 | 171 | 424 | 560 | 0.59 | 101 | 438 |
| 200 | 0.81 | 186 | 419 | 570 | 0.71 | 167 | 434 |
| 210 | 0.89 | 202 | 421 | 580 | 0.64 | 121 | 424 |
| 220 | 0.87 | 227 | 419 | 590 | 0.67 | 156 | 424 |
| 230 | 0.75 | 184 | 424 | 600 | 0.68 | 148 | 422 |
| 240 | 0.68 | 157 | 419 | 610 | 0.61 | 145 | 425 |
| 250 | 1.03 | 133 | 419 | 620 | 0.70 | 155 | 433 |
| 260 | 0.43 | 251 | 419 | 630 | 0.79 | 163 | 423 |
| 270 | 0.83 | 171 | 418 | 640 | 0.58 | 136 | 430 |
| 280 | 1.21 | 154 | 420 | 650 | 0.60 | 115 | 432 |
| 290 | 0.60 | 148 | 420 | 660 | 0.55 | 143 | 431 |
| 300 | 0.60 | 148 | 420 | 670 | 0.55 | 120 | 431 |
| 310 | 0.65 | 158 | 421 | 680 | 0.52 | 130 | 433 |
| 320 | 0.71 | 142 | 420 | 690 | 0.57 | 136 | 435 |
| 330 | 0.74 | 182 | 425 | 700 | 0.47 | 117 | 426 |
| 340 | 0.88 | 203 | 424 | 710 | 0.49 | 122 | 430 |
| 350 | 0.84 | 170 | 424 | 720 | 0.42 | 107 | 432 |
| 360 | 0.80 | 178 | 426 | 730 | 0.40 | 115 | 431 |
| 370 | 0.77 | 171 | 426 | 740 | 0.43 | 113 | 432 |

the mean grain size and higher values of the sorting index is observed between 380 and 280 cmbsf. Above 280 cmbsf, mean grain size is comparatively fine, although somewhat variable, and sorting is more

uniform. The important point is that the rather smooth distribution in the grain size parameters implies an absence of turbidites and other types of mass gravity flows within the studied section of the core.

4.1.4. Inorganic geochemistry

The samples for chemical analysis were selected to span the full range of observed TOC values as well as the parts of the core where the palynofacies and mineralogical data show contrasting values. The elemental compositions are compared after normalizing the trace metal concentrations to Al, a proxy for aluminosilicate detritus (see discussion about Al normalization in Van der Weijden, 2002, and Tribouvillard et al. 2006). In addition, trace metal (TM) concentrations are expressed in terms of enrichment factors (EF_{TM}), where the Al-normalized metal concentration is compared to the average shale values of Wedepohl (1971, 1991): $EF_{TM} = TM/Al_{sample} : TM/Al_{average\ shale}$. When $EF_{TM} > 1$, the trace metal of interest is enriched relative to average shale.

4.1.4.1. Major elements. Table 1 illustrates that the major elements show little variation down core. It indicates that the chemical composition, and therefore the mineralogical nature, of the non-carbonate fraction of the sediment were almost constant through time. The carbonate fraction is also almost invariant (Fig. 3).

4.1.4.2. Trace elements. We emphasized several redox-sensitive and/or sulfide-forming elements along with standard detrital or productivity proxies (see reviews in Algeo and Maynard, 2004; Brumsack, 2006; McManus et al., 2006; Tribouvillard et al., 2006). Mo, U, V, Ni, Co, Cu, and Zn are influenced by the redox status of the base of the water mass and pore waters as well as the amount of OM deposited in the sediment. Tribouvillard et al. (2004a, 2005, 2006) illustrated how Ni and Cu can be used as productivity tracers, as well as the classically used Ba, Th and Zr are governed by the detrital supply only, and Cr may be influenced by the detrital supply and the redox conditions of bottom and pore waters.

Table 1 shows the Al-normalized concentrations of trace metals, as well as the enrichment factors. Some elements show an EF close to one, that is, no enrichment relative to average shale composition: Cu, Ba, V, U and Zr. Molybdenum shows a marked enrichment ($14 < EF_{Mo} < 51$), and Cr and Ni show a moderate enrichment ($1.5 < EF_{Ni} < 4.4$; $2 < EF_{Cr} < 5.7$). Zn and Co are moderately depleted ($0.6 < EF_{Zn} < 0.9$; $0.5 < EF_{Co} < 0.9$).

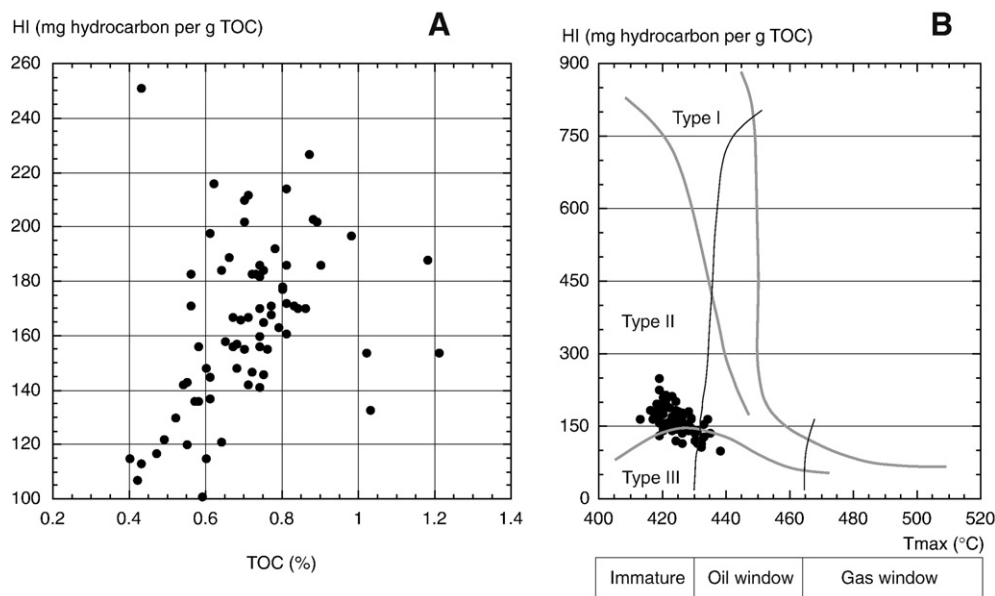


Fig. 4. Rock Eval pyrolysis parameters. A – TOC vs. Hydrogen Index (HI); B – Tmax vs. HI crossplot illustrating the origin and maturation state of the samples. Types I, II and III refer to the origin of OM (in short, lacustrine, marine, land-derived, respectively).

A few observations regarding elemental relationships follow.

- Correlation with Al. Ba, Co, Cu, V, Zn, and Zr show no correlation with Al ($R^2 < 0.01$ for Ba, Co, Cu, Zn and Zr, $R^2 = 0.06$ for V, $n = 10$). Mo, Ni, and Cr show a negative correlation with Al ($R^2 = 0.58, 0.62, 0.60$, respectively, $n = 10$). The fact that these correlations are negative with respect to Al suggests control by a dilution process — that influx of more siliciclastics dilutes organic matter and the trace metals associated with it. U and Th display a good positive correlation with Al ($R^2 = 0.93$ and 0.76 , respectively, $n = 10$), suggesting a most probable clastic origin, contrary to Mo, Ni, and Cr.
- No relationship between Mn and Mo, Ni, and Cr was observed, though Mn redox cycling may be involved in the capture of these elements (Calvert and Pedersen, 1993; Tribovillard et al., 2006).
- No relation was observed between Fe and Ni, Cu, and Mo, evidencing no significant incorporation of the trace metals to iron sulfide.
- Ni and Cu are not correlated ($R^2 = 0.0019$, $n = 10$).
- An excellent correlation is observed between Cr and Ni ($R^2 = 0.97$, $n = 10$), and a good one is drawn between Mo and Cr, and Ni ($R^2 = 0.69$ and 0.65 , respectively, $n = 10$).
- Lastly, TOC is not correlated with any trace metal.

The chemical analysis of the clay fraction may be compared to that of the bulk fraction (Table 1). The Al-normalized concentrations of V, U, Th, Cu, and Co of both the bulk and clay fractions are similar. Conversely, the Al-normalized concentrations of Mo, Cr, and Ni are quite different in that they are much lower in the clay fraction than in the bulk one. It is inferred therefore that the enrichment in Mo, Cr, and Ni observed in the bulk fraction is not related to the non-reactive, $< 2 \mu\text{m}$ (clay) fraction of the land-derived flux and that it most probably reflects authigenic enrichment.

5. Interpretations

5.1. Rock Eval parameters

The vertical distribution of the Rock Eval parameters is not affected by the variations in the abundance of the various classes of figured elements of palynofacies, though these elements are of contrasting chemical composition, which affects both Tmax and HI values. This observation is explained by the overwhelming presence of marine amorphous OM, which mutes the variations of the figured elements. The observed positive correlation between TOC and HI is a classical feature showing that the more abundant the OM, the more aliphatic it is. In other words, the influence of marine OM (i.e., its relative abundance) is larger when TOC increases. Correspondingly, the more aliphatic, the less refractory the OM, hence the negative correlation between HI and Tmax. The decrease in TOC and HI with depth can be attributed to a progressive degradation of OM. The remaining part is gradually enriched in more refractory products as the more labile fraction is preferentially removed, as evidenced by the increase of the Tmax values.

The important point is that the whole data set shows moderate HI values and relatively high Tmax values for a recent organic assemblage dominated by marine-derived AOM. This observation implies that OM throughout the section is noticeably degraded.

5.2. Palynofacies

The figured elements are dominated by land-derived phytoclasts that are refractory constituents and correlatively poor in more labile constituents. This selective enrichment in refractory OM is unexpected for a depositional setting that is close to the Mississippi River mouth, suggesting that OM underwent a marked degradation that removed most of the labile fraction. This interpretation is supported by the absence of fluorescence of the kerogens along with the HI–Tmax parameters discussed above. OM degradation lowered the

aliphaticity, and hence the fluorescence potential (Tyson, 1995). Thus our results independently confirm those of Wong et al. (1985) and Sheu (1990) who concluded that settling OM is trapped at the stable pycnocline long enough to undergo extensive degradation. Incidentally, the relatively extensive degradation of OM could at least partly explain why the rate of bacterially-mediated sulfate reduction is rather low in the Orca Basin. The low rate was reported by Trefry et al. (1984), and Sheu (1990), despite abundant dissolved sulfate and appreciable OM. Sheu (1990) and Sass et al. (2001) discuss the possible limitation of bacterial sulfate-reducing activity by salinity, but according to Porter et al. (2007, and reference therein), high salinity cannot be suspected as the cause of lower sulfate reduction rates. Consequently, it is suggested that refractory OM could not sustain extensive sulfate reduction (which does not preclude any limitation by salinity).

5.3. Inorganic geochemistry

The narrow ranges of variation in the carbonate fraction and major-element concentration profiles underscore the fact that the nature of the inorganic fraction of the sediment is almost invariant. U and Th are positively correlated to Al, which is expected for Th but not for U; this is evidence that the very low concentration of U has a detrital origin and does not record authigenic enrichment. Mo, Ni, and Cr, being negatively correlated to Al, exhibit an enrichment that is “diluted” by the clastic fraction and that must be associated with the organic or authigenic fraction of the sediment (see Lyons and Severmann (2006) for the role of clastics). Zr is not correlated to Al, when measured on the bulk sediment ($R^2 < 0.001$, $n = 10$), but the correlation is better (though only moderately significant) using the Zr concentration of the clay-sized fraction ($R^2 = 0.44$, $n = 10$). This unexpected absence of correlation may be due to the narrow range of Al variation that precludes easy discrimination of subtle differences in coupled Zr content. Alternatively, Zr may be present in a somewhat coarser (silt- or sand-sized) fraction and not associated dominantly with the clay-sized fraction (Jaminski et al., 1998).

Among the redox-sensitive elements, U and V are not enriched whereas Mo is significantly elevated. Mo has never been reported to be enriched without concurrent V and U enrichments for OM-rich sediments or sedimentary rocks deposited under oxygen-deficient depositional conditions. In addition, in moderately reducing environments, U and V are usually more enriched than Mo; in strongly reducing environments, U, V, and Mo are all markedly enriched (Algeo and Maynard, 2004; Tribovillard et al., 2006, and references therein). Under oxygen-deprived conditions, as should be the case for the Orca Basin, U and V form insoluble oxides and hydroxides that are transferred to the sediment. H_2S may play a partial role in the capture of V but plays no role in the capture of U. Thus, the near absence of H_2S in the bottom brines of the Orca Basin cannot explain the lack of enrichment of U and V.

In addition, among the trace metals usually considered as influenced by the OM supply (Ni, Co, Cu and, to a lesser degree Zn), only Ni is enriched, and the enrichment is observed for the bulk fraction, not in the clay fraction. Again, the absence of enrichment for Cu, Co, and Zn is unexpected because the sediment contains appreciable amounts of OM. As recently reported (Piper, 2001; Tribovillard et al., 2004a, 2005, 2006; Piper et al., 2007), in black shales and OM-rich sedimentary rocks, excellent Ni vs. Cu, and TOC vs. Ni or Cu correlations can be observed (Fig. 5), most probably because Ni and Cu were brought to the sediment in association with OM as organometal complexes (e.g., Piper et al., 2007; Perkins et al., in press; see also the papers reviewed in Brumsack, 2006). Fig. 5 shows that for a wide range of sediments and sedimentary rocks containing abundant OM, Ni and Cu are closely related. This correlation seems to be a general feature through time and space, because the formations shown in the figure were deposited in various geologic settings. In the present case,

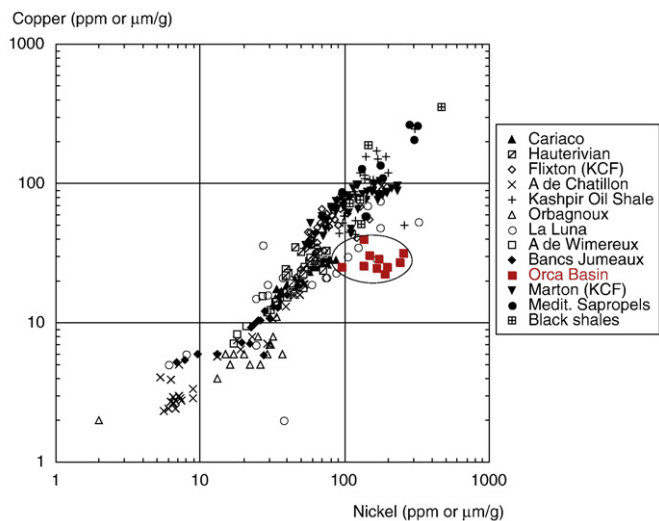


Fig. 5. Nickel abundance vs. Cu abundance for the studied Orca samples and samples from various geological formations and sediments that contain appreciable amounts of OM and that were deposited under oxygen-depleted conditions (suboxic to euxinic). Cariaco: Holocene sediments of the Cariaco Basin offshore Venezuela (Tribouvillard et al., 2004b); Hauterivian: marls of the SE-France Basin, La Charce section, unpublished data; Flixton: samples of the Kimmeridge Clay Formation cored in the Flixton Borehole, Cleveland Basin, UK (Tribouvillard et al., 1994, 2004a, 2005); A de Chatillon: Argiles de Châtillon Formation, Kimmeridgian, Boulonnais coast, France (Tribouvillard et al., 1994, 2001, 2004a, 2005); Kashpir Oil Shales: Kimmeridgian Kashpir Oil Shales Formation, Volgia Basin, Russia (Riboulleau et al., 2003); Orbagnox: Kimmeridgian Laminites bitumineuses Formation at Orbagnox, Jura Mountains, France (Tribouvillard et al., 1991, 2004b; Mongenot et al., 1997); La Luna: Cretaceous La Luna Formation of Venezuela (Mongenot et al., 1996; Tribouvillard et al., 2004b); A de Wimereux: Argiles de Wimereux Formation, Tithonian, Boulonnais coast, France (Tribouvillard et al., 2005); Bancs Jumeaux: Tithonian Banc Jumeaux Fm., Boulonnais coast, France (Tribouvillard et al., 2005, 2008); Marton: samples of the Kimmeridge Clay Formation cored in the Marton Borehole, Cleveland Basin, UK (Tribouvillard et al., 1994, 2004a, 2005); Orca: this study; Medit. Sapropels: Mediterranean sapropels (Nijenhuis et al., 1999); black shales: average values for various black shale formations of Jurassic, Cretaceous and Miocene ages (Nijenhuis et al., 1999, Brumsack, 2006).

the Orca Basin samples diverge from the general trend. This absence of correlation suggests that Ni and Cu accumulation followed different pathways. Either Cu was brought to the sediment but not trapped, or Cu was not present in abundance in the brine. In the former case, if Cu had been brought in association with OM, it could have reacted with sulfides. Cu is known to have a high potential for incorporation into pyrite (Morse and Luther, 1999) but the low abundance of pyrite would have prevented Cu capture and retention. However, Cu could have theoretically reacted with the abundant FeS through adsorption and/or incorporation (see details about the complex behavior of Cu toward sulfide species in Morse and Luther, 1999) but no correlation is observed between Fe and Cu. Thus the absence of Cu enrichment is rather interpreted as reflecting low Cu availability in the Orca Basin brine. Cu was perhaps not scavenged in large amounts by the much-degraded settling OM. Organic matter may have incorporated Cu prior to and during settling through the upper part of the water mass but Cu would have been released during the extensive decay undergone by OM at the pycnocline (e.g., Sunda, 1995). In the end, the amount of Cu delivered by OM to the sediment was low and not in proportion with TOC. Conversely Ni was transferred to the sediment but it is also not correlated with TOC, which suggests that Ni was not enriched through OM inputs (like Cu). Another enrichment mechanism must be envisioned.

To sum up, we observe an unexpected absence of enrichment for U, V and Cu (also for Co and Zn – not discussed here), but we observe strong enrichment in Mo, and weak enrichment in Cr, and Ni. Lastly, Ni and Cu are decoupled, which is unusual for OM-hosting sediments or sedimentary rocks (e.g., Rutten and de Lange, 2003). In what follows, we try to explain this paradoxical situation.

5.3.1. A possible basin reservoir effect in the Orca Basin?

To account for the absence of U, V and Cu enrichment in the presence of nontrivial enrichment in Mo, Cr, and Ni, we can invoke the “basin reservoir effect” described by Algeo and Lyons (2006) for several modern anoxic marine environments: when a strong pycnocline induces dramatic isolation of the deep-water mass, the inventory of dissolved trace metals could become depleted as the sink flux of trace metals to the sediments exceeds the input associated with deep-water renewal. Weber and Sackett (1981) already mentioned how U concentration in the brines can be limited in the absence of mixing and diffusion across the density gradient. In other words, in the case of a “basin reservoir effect”, the restricted water mass progressively grows depleted in some dissolved trace metals, which prevents any further authigenic enrichment of sediments, contrary to expectation. In the Orca Basin, the anoxic brine pool has a volume of $\sim 5 \text{ km}^3$, compared to the $\sim 5000 \text{ km}^3$ volume of the anoxic pool of the Cariaco Basin (that is, the water mass volume below the 300 m depth). In other words, a basin reservoir effect was observed for the Cariaco Basin despite an anoxic compartment that is 1000 times larger than that of the Orca Basin. In addition, the pycnocline of the Orca Basin is more stable than the pycnocline of the Cariaco Basin, because of the dramatic density contrast induced by the brines, and thus exchange with overlying waters is strongly inhibited. Wiesenburg et al. (1985) reported an Orca brine residence time of ca. 5700 yr, whereas Addy and Behrens (1980) estimated that the brine began to flow into the basin 7900 yr BP. Thus the brine in the Orca Basin is much older than the 800 yr residence time for the deep water of the Cariaco Trench or the 2000 yr residence time for bottom water of the Black Sea (Wiesenburg et al., 1985). It is inferred that limited metal inventory must play an important role in the dissolved-trace metal depletion of the small subpycnoclinical reservoir of the Orca Basin. Such depletion is indeed observed for several trace metals such as U and V (Eric Viollier, personal communication, 2007; data to be published): the brines contain $< 10\%$ of the dissolved U and V of undepleted seawater. Under these conditions, the positive correlation between Mo, Ni, and Cu contents and TOC that is typically observed in anoxic depositional systems may be absent, and the appreciable capture of dissolved U and V may not be possible, even under theoretically favorable (i.e., strongly reducing) conditions. Dissolved U and V concentrations being very low in the brine, significant U and V authigenic enrichment is not possible and the only carrier phase of U and V to the sediment is the terrigenous input. Under these conditions, the enrichment factor of U and V relative to average shale is logically equal or close to 1.

5.3.2. How to explain the Mo, Cr and Ni enrichment?

A marked Mo enrichment and a more modest one in Cr and Ni are observed. A first explanation could be a marked input of Cr–Ni enriched land-derived particles. Mo is usually present in crustal rocks in such low abundance that such an enrichment may be ruled out. In addition, as mentioned above in Section 3.2, the land-derived supply delivered by the Mississippi River to the Gulf of Mexico is close to average shale from a geochemical composition point of view (Swarzenski et al., 2008). Thus a Cr–Ni enrichment due to some ultramafic rocks in the drainage system cannot be suspected. In addition, neither Cr nor Ni shows a good correlation with Al, which is considered here as a good proxy for the detrital signal. The R^2 values for Cr and Ni vs. Al are 0.60 and 0.61 respectively, and the correlation is negative. In other words, the Cr and Ni contents seem to be diluted by the Al-bearing fraction of the sediment. To strengthen this statement, it is observed that Cr and Ni are not correlated either with Th or Ti, which are also proxies for the land-derived fraction. Consequently, the observed Cr and Ni enrichment cannot be attributed to the clastic supply.

It follows that the enrichment in Mo, Cr and Ni observed here may have an organic or authigenic origin. First, some considerations about the geochemistry of Mo, Cr and Ni are discussed below.

5.3.2.1. Molybdenum. Many models for Mo enrichment call upon Mo reduction or coupling to the redox cycle of Mn, with Mo being scavenged directly from the water column or captured from pore waters supplied diffusively with Mo from the overlying water column (Berrang and Grill, 1974; François, 1988; Emerson and Husted, 1991; Huerta-Diaz and Morse, 1992; Calvert and Pedersen, 1993; Crusius et al., 1996; Zheng et al., 2000; synthesized in Tribouillard et al., 2006). Other models favor a direct role played by sulfide. For example, Helz et al. (1996) and Vorlicek et al. (2004) suggested that fixation in the presence of dissolved sulfide does not simply result from MoS_2 or MoS_3 formation, but instead mineralization occurs through organic thiomolybdates and inorganic Fe–Mo–S cluster complexes possibly occurring as solid-solution components in Fe sulfides. Helz et al. (1996) introduced the concept of a geochemical switch, through which dissolved sulfide (dominated by HS^- at circumneutral pH) transforms Mo from a largely conservative element to a particle-reactive species in marine depositional environments (this view was later complemented by Zheng et al. (2000) who suggest that two switches may exist). The oxygen atoms in MoO_4^{2-} are susceptible to replacement by soft ligands, such as S donors. According to Erickson and Helz (2000) and Helz et al. (2004), a key step in this inorganic pathway is the reaction: $\text{MoO}_4^{2-} \rightarrow$ thiomolybdates ($\text{MoO}_x\text{S}_{4-x}$, $x=0-3$), which are particle reactive and thus prone to scavenging. The sulfide activation of the switch depends on $\Sigma\text{H}_2\text{S}$ activity (Erickson and Helz, 2000; Zheng et al., 2000). Because each successive sulfidation reaction is about one order of magnitude slower than the previous one, dithio- \rightarrow trithio- and trithio- \rightarrow tetra-thiomolybdate equilibria might not be achieved in seasonally or intermittently sulfidic waters (Erickson and Helz, 2000). Persistently sulfidic conditions seem to be required. In the sediments, the transformation reactions are catalyzed by proton donors or in the presence of some active-surface minerals such as kaolinite (Erickson and Helz, 2000; Vorlicek and Helz, 2002). Once the thiomolybdate switch has been achieved, Mo is scavenged by forming bonds with metal-rich (notably Fe) particles, sulfur-rich organic molecules (Helz et al., 1996, 2004; Tribouillard et al., 2004b), and iron sulfide (Vorlicek et al., 2004). The work by Helz et al. (1996) also suggests the formation of compact, monocrystalline Fe–Mo–S cluster compounds that are capable of surviving over geologic time periods. Bostick et al. (2003) showed that the clusters are retained on pyrite surfaces, and Vorlicek et al. (2004) argued that a Mo reduction step is favorable, if not necessary, in that case.

To sum up, usually, Mo may be enriched in the sediment owing to Mn redox cycling, incorporation by settling OM and/or pyrite. In addition to these three mechanisms, H_2S in pore waters plays an important role, as witnessed by enrichments seen beneath oxygen-poor but nonsulfidic (suboxic) bottom water, but persistently sulfidic bottom-water conditions seem to be required for large enrichment (McManus et al., 2006). In the present case, no correlation is observed between Mo and Mn, TOC, and Fe contents, which suggests that none of the three mechanisms dominates. The Mn redox cycling is active in the Orca Basin but it occurs within the water column, in the transition zone between normal normal-marine water and underlying brines (Trefry et al., 1984; Van Cappellen et al., 1998). Consequently, Mn redox cycling cannot account for direct Mo enrichment of the sediment. The Mo enrichments are too large to be accounted for by an organic host phase, given that TOC concentrations are <1%. In addition, the very low abundance of H_2S observed presently in the water column strongly suggests that the H_2S switch must not operate steadily in the Orca Basin. Nevertheless, it is possible that sporadic episodes of elevated H_2S might have occurred in the basin during the Holocene (e.g., Sheu and Presley, 1986) and could have activated the switch temporarily.

5.3.2.2. Chromium. In the present study, Cr and Ni show some authigenic enrichment, and the abundances of both elements are closely correlated, whereas Ni and Cu are decoupled, contrary to common

observations in black shales and OM-rich sedimentary rocks (Fig. 5; see also Rutten and De Lange, 2003). Usually, Cr may be transported to the sediment in two ways (e.g., Breit and Wanty, 1991; Piper, 1994; Dean et al., 1997; Piper, 2001; Piper and Perkins, 2004; Algeo and Maynard, 2004; see reviews in Brumsack, 2006, and Tribouillard et al., 2006 and references therein). First, it can be delivered with the land-derived clastic fraction (e.g., chromite, clay minerals, and ferromagnesian minerals in which Cr substitutes readily for Mg). Second, chromium is present in oxygenated seawater primarily as Cr(VI) in the chromate anion, CrO_4^{2-} , and to a much lesser extent as Cr(III) in the aquahydroxyl ion, $\text{Cr}(\text{H}_2\text{O})_4(\text{OH})^{2+}$, with an average concentration of 4.04 nmol/kg and a residence time of 8 kyr (Tribouillard et al., 2006). Under normal seawater conditions, the chromate anion is soluble, but under anoxic conditions, Cr(VI) is reduced to Cr(III), forming aquahydroxyl cations and hydroxyl cations [$\text{Cr}(\text{OH})^{2+}$, $\text{Cr}(\text{OH})_3$, $(\text{Cr, Fe})(\text{OH})_3$], which can readily complex with humic/fulvic acids or adsorb to Fe- and Mn-oxyhydroxides. Thus, Cr is exported to the sediments. Because of structural and electronic incompatibilities with pyrite, Cr(III) uptake by authigenic Fe sulfides is very limited. In addition, Cr is not known to form an insoluble sulfide (Huerta-Diaz and Morse, 1992). Consequently, upon OM remineralization by sulfate-reducing bacteria, Cr is not readily trapped within the sediments in the form of a sulfide and may be lost to the overlying water column by diffusive/advective transport during sediment compaction. In the case of the Orca Basin, the anoxic conditions prevailing in the brine could foster the formation of aquahydroxyl and hydroxyl cations but their transfer to sediment must be hampered by (1) the poor preservation state of OM (that could not fix Cu), and (2) the fact that the Me–Fe redox cycling operates at the seawater–brine interface (which also limits Mo transfer).

5.3.2.3. Nickel. In oxic marine environments, Ni behaves as a micronutrient and may be present as soluble Ni^{2+} cations or NiCl^+ ions but it is mostly present as a soluble Ni carbonate (NiCO_3) or adsorbed onto humic and fulvic acids (Algeo and Maynard, 2004; Brumsack, 2006; Tribouillard et al., 2006, and references therein). Complexation of Ni with OM will accelerate scavenging in the water column and thus sediment enrichment. Upon OM decay, Ni may be released from organometallic complexes to pore waters. In moderately reducing sediments, Ni is cycled from the sediment into the overlying waters because sulfides and Mn oxides are absent. Under (sulfate-) reducing conditions, Ni may be incorporated as the insoluble NiS into pyrite (as a solid solution), even if the kinetics of the process are slow. In the case of the Orca Basin, once again, the poor preservation state of OM must have strongly limited Ni transfer to sediment. Furthermore, the negligible presence of pyrite could not act as a trap for Ni (that cannot either form its own sulfides under usual sedimentary conditions).

To sum up, the observed enrichment in Mo, Cr and Ni has no straight-forward explanation. The simpler hypothesis involves H_2S as a mediator. In seawater, the presence of H_2S induces the reduction of soluble forms of Cr(VI) to insoluble forms of Cr(III). The presence of dissolved metals such as Ni, Pb, Cu and Cd has been observed to cause large increases in the reduction rate of Cr(VI) at micromolar concentrations (Pettine et al., 1998). The effect can be accounted for by the formation of MeCrO_4 complexes that react faster with sulfide than free chromate. This effect is much more pronounced with Ni than Cu (Pettine et al., 1998), which can explain the excellent Ni–Cr correlation and the absence of correlation between Cu and Cr. Thus, the Ni–Cr enrichment may be attributed to reduction reactions induced by the sporadic occurrence of H_2S that also activated the H_2S switch, leading to Mo enrichment.

Thus the scheme by Pettine et al. (1998) accounts for enrichment in Cr and Ni, the fact that Cr is more enriched than Ni, and that Ni and Cu are decoupled. The chemical mechanism of the scheme does not involve Mo directly but does require sporadic occurrences of H_2S that have in turn a possible impact on Mo precipitation. This incidental

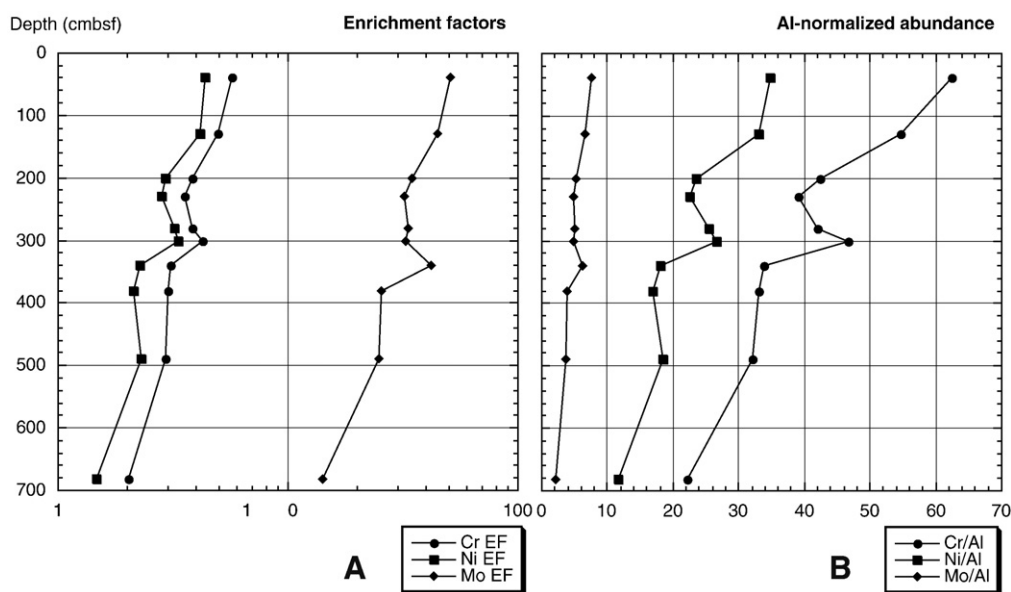


Fig. 6. Stratigraphic distribution of the enrichment factors (A) and Al-normalized abundance (B) for Cr, Ni and Mo. Since Al is expressed in weight % and trace metals are expressed in ppm or $\mu\text{g/g}$, the values of the trace metal to aluminum ratios are multiplied by 10^4 .

impact may explain why the Cr vs. Mo and Ni vs. Mo correlations are not as strong as Ni vs. Cr.

5.3.3. Episodic H_2S enrichment

In a basin such as the Orca characterized by its peculiar geodynamic context (salt diapirs and tectonics), the occurrence of H_2S in the water column has two possible origins: (1) in situ bacterial sulfate reduction and (2) diffusion from underlying sulfidic pore waters. The sulfate reduction rate is known to be low in the Orca Basin but sulfate concentration is not limiting (Sheu and Presley, 1986; Van Cappellen et al., 1998; Hurtgen et al., 1999). In addition, we discuss above the fact that the rate of sulfate reduction may be lowered by the relatively poor preservation state of OM (see Section 5.2). Thus, increased bacterially mediated sulfate reduction in the water column implies an increased influx of labile OM to the base of the water column. Such an increased flux of OM may be caused by an increase in surface production or a disruption of the pycnocline and the subsequent sinking of the biomass usually lying at the pycnocline (however the OM may be strongly degraded after a stay at the pycnocline and, consequently, lowly reactive). Nevertheless, TOC does not correlate significantly with Ni (Ni/Al, NiEF); such an enhanced organic input presumably would be accompanied by increased proportions of Ba, Ni and Cu, and in that case, we see no reason why Ni and Cu would be decoupled. Furthermore, the Orca brines are rich in sulfate from the leaching of evaporite-bearing diapirs and the sulfate reduction rate is low. Thus, barite dissolution must not occur and Ba should correlate with TOC as related to varying levels of productivity, unless barite is completely solubilized at the pycnocline or during the OM settling above the pycnocline, which is improbable. Consequently, we see no compelling evidence that the H_2S content increased via enhanced bacterial sulfate reduction.

Another scenario is possible to account for sporadic injections of dissolved H_2S from the transition zone in the water column down to the brines (Sheu and Presley, 1986). As hypothesized by these authors, variations in mixing at the brine–seawater interface – where dissolved H_2S is present in appreciable amounts – are possible, as storms, winter cold fronts, etc. could set up internal waves in the basin.

Lastly, as reported in Section 2, the brines did not originate beneath the Orca Basin but instead were introduced from somewhere outside. Nevertheless, it is possible that an alternative source of H_2S could be

released along faults created by the buoyant movements of salt diapirs that control basin geometry as observed elsewhere in the Gulf of Mexico (e.g., Gilhooly et al., 2007). Such release of H_2S could play a modest role in the capture of Cr and Ni, as well as Mo. This activity could also be involved in the occasional episodes of pyrite formation observed in some cores (Sheu and Presley, 1986; Hurtgen et al., 1999). Such H_2S releases linked to salt diapir dynamics are observed in other places in the Gulf of Mexico but remain speculative in the case of the Orca Basin in the absence of pore water data.

5.3.4. Progressive enrichment of Mo, Cr and Ni?

Fig. 6 shows that the Al-normalized concentration and the enrichment factors of Mo, Cr, and Ni decrease with increasing depth below sea floor. The stratigraphic distribution may be viewed as a progressive upward enrichment of the sediment in Mo, Ni, and Cr: the younger the sediment, the richer the three trace metals. In the absence of data about the pore water chemistry and sufficient information about the chemistry of the trace metal carrier phases, the controls on these trace metal profiles remain unknown. However, the up-section increases are consistent with (1) increasing TOC and (2) increasing HI, both of which suggest more intense anoxia in Orca Basin deep waters toward the present, allowing accumulation of larger quantities of labile OM. More intense anoxia could account for the vertical profiles in Cr, Ni, and Mo.

6. Conclusion

Our study of the palynofacies assemblage and its co-variations with the clay–mineral assemblage reveals the appreciable influence by land-derived inputs to the Orca Basin, though the marine-produced organic fraction is dominant. Though the anoxic bottom conditions should favor preservation, OM is rather degraded in the Orca Basin sediments and its degradation must be accounted for, at least in part, by extended residence at the stable brine–sea water interface at 2230–2250 m water depth, where OM is subjected to oxic conditions. The degradation deduced from the release of abundant biogenic iodine at the pycnocline (Wong et al., 1985) is confirmed by the relatively low HI–high Tmax values and the non-fluorescence of the kerogens found within the sediment at all levels, including at the sediment–water interface.

Our results confirm that the sediments of the Orca Basin do not show strong enrichments of trace metals (except for Mo), although the

permanently anoxic bottom waters and the OM flux would be expected to induce the capture of redox- and OM-sensitive trace metals. We suggest that the non-enrichment in U and V could be explained by the basin reservoir effect of Algeo and Lyons (2006), whereby an expected low metal inventory within the restricted deep-water mass limits the quantity taken up by the sediment. The non-enrichment in Cu could reflect the same condition, plus the relatively degraded OM may not readily form organometallic complexes. However a marked enrichment is observed for Mo, along with a modest enrichment in Ni, and Cr, which could be accounted for by sporadic increases in dissolved sulfide content. The episodic occurrences of H₂S would not be sufficient to promote a detectable FeS to FeS₂ conversion, but they would induce the capture of Mo (thiomolybdate) and, to a lesser extent, Ni–Cr (as Ni–CrO₄ complexes). Thus our trace metal results, though preliminary, suggest several potentially important scenarios. Rather than multiplying bulk sediment analyses, we definitely need now data about the trace metal chemistry of the brines compared to the overlying normal-marine water mass and of the pore water composition.

Our results also suggest that the observed relationship between Ni and Cu could help in interpretations of paleodepositional conditions elsewhere. In sediments containing appreciable amounts of OM and deposited under oxygen-poor bottom conditions, a positive correlation is expected between Ni and Cu that are delivered together to the sediments with OM and retained by OM and iron sulfide (pyrite). If Ni and Cu are decoupled, with a relative enrichment of Ni compared to Cu, and if depositional conditions are independently constrained as reducing, it is suggested that the reducing conditions might not be due solely to usual oxygen consumption through OM decay but may also be accounted for by another mechanism, such as a H₂S release from basin basement. A test of this hypothesis must be carried out with other brine-rich basins.

Acknowledgements

We thank Yvon Balut, the Institut Paul-Emile Victor (IPEV), the crew of the *Marion-Dufresne R/V* and the IMAGES program for core collection. We thank the technical staff of the Géosystèmes lab: Léa-Marie Emaile, Laurence Debeauvais, Deny Malengros & Philippe Recourt. We thank Gert J. De Lange for his work as an Editor-in-Chief and the two anonymous referees that helped us improve significantly our paper.

References

- Addy, S.K., Behrens, E.W., 1980. Time of accumulation of hypersaline anoxic brine in Orca basin (Gulf of Mexico). *Mar. Geol.* 37, 241–252.
- Algeo, T.J., Maynard, J.B., 2004. Trace-element behavior and redox facies in core shales of Upper Pennsylvanian Kansas-type cyclothems. *Chem. Geol.* 206, 289–318.
- Algeo, T.J., Lyons, T.W., 2006. Mo–total organic carbon covariation in modern anoxic marine environments: implications for analysis of paleoredox and paleohydrographic conditions. *Paleoceanography* 21, PA1016. doi:10.1029/2004PA001112.
- Baudin, F., Tribouillard, N., Laggoun-Defarge, F., Lichtfouse, E., Monod, O., Gardin, S., 1999. Depositional environment of a Kimmeridgian carbonate “black band” (Akkuyu Fm., SW Turkey). *Sedimentology* 46, 589–602.
- Berrang, P.G., Grill, E.V., 1974. The effect of manganese oxide scavenging on molybdenum in Saanich Inlet, British Columbia. *Mar. Chem.* 2, 125–148.
- Bostick, B.C., Fendorf, S., Helz, G.R., 2003. Differential adsorption of molybdate and tetrathiomolybdate on pyrite (FeS₂). *Environ. Sci. Technol.* 37, 285–291.
- Breit, G.N., Wanty, R.B., 1991. Vanadium accumulation in carbonaceous rocks: a review of geo-chemical controls during deposition and diagenesis. *Chem. Geol.* 91, 83–97.
- Brooks, J.M., Wiesenburg, D.A., Roberts, H., Carney, R.S., MacDonald, I.R., Fisher, C.R., Guinasso Jr., N.L., Sager, W.W., McDonald, S.J., Burke Jr., R.A., Aharon, P., Bright, T.J., 1990. Salt, seeps and symbiosis in the Gulf of Mexico. A preliminary report of deepwater discoveries using DSV Alvin. *Eos, Trans. Am. Geophys. Union* 71, 1772–1773.
- Brumsack, H.-J., 2006. The trace metal content of recent organic carbon-rich sediments: implications for Cretaceous black shale formation. *Palaeogeogr., Palaeoclimat., Palaeoecol.* 232, 344–361.
- Calvert, S.E., Pedersen, T.F., 1993. Geochemistry of Recent oxic and anoxic sediments: implications for the geological record. *Mar. Geol.* 113, 67–88.
- Carignan, J., Hild, P., Morel, J., Yeghicheyan, D., 2001. Routine analysis of trace elements in geochemical samples using flow injection and low-pressure on-line liquid chromatography coupled to ICP-MS: a study of geochemical reference materials BR, DR-N, UB-N, AN-G and GH. *Geostand. Newslett.* 25, 187–198.
- Crusius, J., Calvert, S., Pedersen, T., Sage, D., 1996. Rhenium and molybdenum enrichments in sediments as indicators of oxic, suboxic, and sulfidic conditions of deposition. *Earth Plan. Sci. Lett.* 145, 65–78.
- Davies, D.K., Moore, W.R., 1970. Dispersal of Mississippi sediment in Gulf-of-Mexico. *J. Sedim. Petrol.* 40, 339–349.
- Dean, W.E., Gardner, J.V., Piper, D.Z., 1997. Inorganic geochemical indicators of glacial-interglacial changes in productivity and anoxia on the California continental margin. *Geochim. Cosmochim. Acta* 61, 4507–4518.
- Emerson, S.R., Husted, S.S., 1991. Ocean anoxia and the concentration of molybdenum and vanadium in seawater. *Mar. Chem.* 34, 177–196.
- Erickson, B.E., Helz, G.R., 2000. Molybdenum (VI) speciation in sulfidic waters: stability and lability of thiomolybdates. *Geochim. Cosmochim. Acta* 64, 1149–1158.
- Espitalié, J., Deroo, G., Marquis, F., 1986. La pyrolyse Rock Eval et ses applications. Part B. *Rev. Inst. Franç. Pétrol.* 40, 755–784.
- Espitalié, J., 1993. Rock Eval pyrolysis. In: Bordenave, M.L. (Ed.), *Applied Petroleum Geochemistry*. Technip, Paris, pp. 237–261.
- Flocks, J., Swarzenski, P., 2007. Sediment collection from Orca and Pigmy Basins, Gulf of Mexico, and analyses for texture and trace-metal concentrations, July 2002, PAGE 127 Campaign. In: Winters, W.J., Lorenson, T.D., Paull, C.K. (Eds.), *Initial Report of the IMAGES VIII/PAGE 127 Gas Hydrate and Paleoclimate Cruise on the RV Marion Dufresne in the Gulf of Mexico, 2–18 July 2002*. U.S. Geological Survey Open-File Report 2004-1358, one DVD. online at <http://pubs.usgs.gov/of/2004/1358/>.
- François, R., 1988. A study on the regulation of the concentrations of some trace metals (Rb, Sr, Zn, Pb, Cu, V, Cr, Ni, Mn and Mo) in Saanich Inlet sediments, British Columbia, Canada. *Mar. Geol.* 83, 285–308.
- Gilhooley III, W.P., Carney, R.S., Macko, S.A., 2007. Relationships between sulfide-oxidizing bacterial mats and their carbon sources in northern Gulf of Mexico cold seeps. *Org. Geochem.* 38, 380–393.
- Gorin, G.E., Steffen, D., 1991. Organic facies as a tool for recording eustatic variations in marine fine-grained carbonates – example of the Berriasian stratotype at Berrias (Ardeche, SE France). *Palaeogeogr., Palaeoclimatol., Palaeoecol.* 85, 303–320.
- Helz, G.R., Miller, C.V., Charnock, J.M., Mosselmans, J.L.W., Patrick, R.A.D., Garner, C.D., Vaughan, D.J., 1996. Mechanisms of molybdenum removal from the sea and its concentration in black shales: EXAFS evidences. *Geochim. Cosmochim. Acta* 60, 3631–3642.
- Helz, G.R., Vorlicek, T.P., Kahn, M.D., 2004. Molybdenum scavenging by iron monosulfide. *Environ. Sci. Technol.* 38, 4263–4268.
- Huerta-Diaz, M.A., Morse, J.W., 1992. Pyritisation of trace metals in anoxic marine sediments. *Geochim. Cosmochim. Acta* 56, 2681–2702.
- Hurtgen, M.T., Lyons, T.W., Ingall, E.D., Cruse, A.M., 1999. Anomalous enrichments of iron monosulfide in euxinic marine sediments and the role of H₂S in iron sulfide transformations: examples from Effingham Inlet, Orca Basin, and the Black Sea. *Am. J. Sci.* 299, 556–588.
- Innocent, C., Fagel, N., Stevenson, R.K., 1999. Do leaching experiments in deep-sea clays isolate a seawater component? *Can. J. Soil. Sci.* 79, 707–713.
- Jaminski, J., Algeo, T.J., Maynard, J.B., Hower, J.C., 1998. Climatic origin of dm-scale compositional cyclicity in the Cleveland Member of the Ohio Shale (Upper Devonian), Central Appalachian Basin, USA. In: Schieber, J., Zimmerle, W., Sethi, P.S. (Eds.), *Shales and Mudstones, v. 1*. Schweizerbart'sche, Stuttgart, pp. 217–242.
- Lallier-Vergès, E., Bertrand, P., Desprairies, A., 1993a. Organic matter composition and sulfate reduction intensity in Oman Margin sediments. *Mar. Geol.* 112, 57–69.
- Lallier-Vergès, E., Bertrand, P., Huc, A.Y., Büchel, D., Tremblay, P., 1993b. Control of the preservation of organic matter by productivity and sulphate reduction in Kimmeridgian shales from Dorset (UK). *Mar. Pet. Geol.* 10, 600–605.
- Lallier-Vergès, E., Hayes, J., Tribouillard, N., Zaback, D., Connan, J., Bertrand, P., 1997. Productivity-induced cyclic sulfur enrichment of hydrocarbon-rich sediments from the Kimmeridge Clay Formation. *Chem. Geol.* 134, 277–288.
- Lyons, T.W., Severmann, S., 2006. A critical look at iron paleoredox proxies: new insights from modern euxinic marine basins. *Geochim. Cosmochim. Acta* 70, 5698–5722.
- McManus, J., Berelson, W.B., Severmann, S., Poulson, R.L., Hammond, D.E., Klinkhammer, G.P., Holm, C., 2006. Molybdenum and uranium geochemistry in continental margin sediments: paleoproxy potential. *Geochim. Cosmochim. Acta* 70, 4643–4662.
- Mongenot, T., Tribouillard, N., Desprairies, A., Lallier-Vergès, E., Laggoun-Defarge, F., 1996. Trace elements as paleoenvironmental markers in strongly mature hydrocarbon source rocks: the Cretaceous la Luna Formation of Venezuela. *Sedim. Geol.* 103, 23–37.
- Mongenot, T., Boussafir, M., Derenne, S., Lallier-Vergès, A., Largeau, C., Tribouillard, N., 1997. Sulphur-rich organic matter from Bituminous Laminites of Orbagnoux (France, upper Kimmeridgian) – the role of early vulcanization. *Bull. Soc. Géol. Fr.* 168, 331–341.
- Morse, J.W., Luther III, G.W., 1999. Chemical influences on trace metal–sulfide interactions in anoxic sediments. *Geochim. Cosmochim. Acta* 63, 3373–3378.
- Nijenhuis, I.A., Bosch, H.-J., Sinnighe, Damsté, J.S., Brumsack, H.-J., De Lange, G.J., 1999. Organic matter and trace element rich sapropels and black shales: a geochemical comparison. *Earth Planet. Sci. Lett.* 169, 277–290.
- Perkins, R.B., Piper, D.Z., Mason, C.E., in press. Oceanography of the Devonian–Mississippian Ap-palachian Basin-trace elements in the Ohio/Sunbury Shales. *Palaeogeogr., Palaeoclimat., Palaeoecol.* doi:10.1016/j.palaeo.2008.04.012.
- Pettine, M., Barra, I., Campanella, L., Millero, F.J., 1998. Effect of metals on the reduction of chromium (VI) with hydrogen sulfide. *Water Research*, 32 1998, 2807–2813.
- Piper, D.Z., 1994. Seawater as the source of minor elements in black shales, phosphorites and other sedimentary rock. *Chem. Geol.* 114, 95–114.
- Piper, D.Z., 2001. Marine chemistry of the Permian Phosphoria Formation and Basin, Southeast Idaho. *Econ Geol* 96 (3), 599–620.

- Piper, D.Z., Perkins, R.B., 2004. A modern vs. Permian black shale – the hydrography, primary productivity, and water-column chemistry of deposition. *Chem. Geol.* 206, 177–197.
- Piper, D.Z., Perkins, R.B., Rowe, H.D., 2007. Rare-earth elements in the Permian Phosphoria Formation: paleo proxies of ocean geochemistry. *Deep-Sea Res.* 54, 1396–1413.
- Porter, D., Roychoudhury, A.N., Cowan, D., 2007. Dissimilatory sulfate reduction in hypersaline coastal pans: activity across a salinity gradient. *Geochim. Cosmochim. Acta* 71, 5102–5116.
- Presley, B.J., Stearns, S., 1986. Interstitial water chemistry. *Deep Sea Drilling Project Leg 961*. In: Bouma, A.H., Coleman, J.M., Meyer, A.W., et al. (Eds.), *Init. Repts. DSDP*, 96. U. S. Govt. Printing Office, Washington, pp. 697–709.
- Riboulleau, A., Baudin, F., Deconinck, J.-F., Derenne, S., Largeau, C., Tribouvillard, N., 2003. Depositional conditions and organic matter preservation pathways in an epicontinental environment: the Upper Jurassic Kashpir Oil Shales (Volga Basin, Russia). *Palaeogeogr., Palaeoclimatol., Palaeoecol.* 197, 171–197.
- Roncaglia, L., Kujper, A., 2006. Revision of the palynofacies model of Tyson (1993) based on recent high-latitude sediments from the North Atlantic. *Facies* 52 (1), 19–39. doi:10.1007/s10347-005-0028-y.
- Rutten, A., de Lange, G.J., 2003. Sequential extraction of iron, manganese and related elements in S1 sapropel sediments, eastern Mediterranean. *Palaeogeogr., Palaeoclimatol., Palaeoecol.* 190, 79–101.
- Sass, A.M., Sass, H., Coolen, M.J.L., Cypionka, H., Overmann, J., 2001. Microbial communities in the chemocline of a hypersaline deep-sea basin (Urania basin, Mediterranean Sea). *Appl. Environ. Microbiol.* 67 (12), 5392–5402.
- Schiff, J., 2007. Alkali elements (Na, K, Rb) and alkaline earth elements (Mg, Ca, Sr, Ba) in the anoxic brine of Orca Basin, northern Gulf of Mexico. *Chem. Geol.* 243, 255–274.
- Sebag, D., Copard, Y., Di-Giovanni, Ch., Durand, A., Laignel, B., Ogier, S., Lallier-Vergès, E., 2006. Palynofacies as useful tool to study origins and transfers of particulate organic matter in recent terrestrial environments: synopsis and prospects. *Earth-Sci. Rev.* 79, 241–259.
- Sheu, D.-D., 1990. The anoxic Orca Basin (Gulf of Mexico): geochemistry of brines and sediments. *Rev. Aquat. Sci.* 2, 491–507.
- Sheu, D.-D., Presley, B.J., 1986. Variations of calcium carbonate, organic carbon and iron sulfides in anoxic sediment from the Orca Basin, northern Gulf of Mexico. *Mar. Geol.* 70, 103–118.
- Sheu, D.-D., Shakur, A., Pigott, J.D., Wiesenburg, D.A., Brooks, J.M., Krouse, H.R., 1987. Sulfur and oxygen isotopic compositions of dissolved sulfate in the Orca Basin: implications for origin of the high-salinity brine and oxidation of sulfides at the brine-seawater interface. *Mar. Geol.* 78, 303–310.
- Shokes, R.F., Trabant, P.K., Presley, B.J., Reid, D.R., 1977. Anoxic, hypersaline basin in the northern Gulf of Mexico. *Science* 196, 1443–1446.
- Sionneau, T., Bout-Roumazielles, V., Biscaye, P.E., van Vliet-Lanoë, B., Bory, A., submitted for publication. Clay mineral distribution over the north American continent and Northern Gulf of Mexico: sources, transportation patterns and depositional processes. *Quarter. Sci. Rev.*
- Sunda, W.G., 1995. The influence of nonliving organic matter on the availability and cycling of plant nutrients in seawater. In: Zepp, R.G., Sonntag, C. (Eds.), *Role of Nonliving Organic Matter in the Earth's Carbon Cycle*. John Wiley and Sons Ltd., pp. 191–207.
- Swarzenski, P.W., Campbell, P.L., Osterman, L.E., Poore, R.Z., 2008. A 1000-year sediment record of recurring hypoxia off the Mississippi River: the potential role of terrestrially-derived organic matter inputs. *Mar. Chem.* 109, 130–142.
- Trabant, P.K., Presley, B.J., 1978. Orca Basin, anoxic depression on the continental slope, northwest Gulf of Mexico. In: Bouma, A.H., Moore, G.T., Coleman, J.M. (Eds.), *Framework, Facies, and Oil-Trapping Characteristics of the Upper Continental Margin: American Association Petroleum Geologists Studies in Geology*, 7, pp. 303–316.
- Trefry, J.H., Presley, B.J., Keeney-Kennicutt, W.L., Trocine, R.P., 1984. Distribution and chemistry of manganese, iron, and suspended particulates in Orca Basin. *Geo-Mar. Lett.* 4, 125–130.
- Tribouvillard, N., Gorin, G., 1991. Organic facies of the early Albian Niveau Paquier, a key black shale level of the Marnes Bleues Formation in the Vocontian Trough (Subalpine Ranges, SE-France). *Palaeogeogr., Palaeoclim., Palaeoecol.* 85, 227–237.
- Tribouvillard, N.-P., Gorin, G., Hopfgartner, G., Manivit, H., Bernier, P., 1991. Conditions de dépôt et matière organique en milieu lagunaire d'âge kimméridgien du Jura méridional français (résultats préliminaires). *Ecol. Geol. Helv.* 84, 441–461.
- Tribouvillard, N., Desprairies, A., Lallier-Vergès, E., Moureau, N., Ramdani, A., Ramanampisoa, L., 1994. Geochemical study of organic-rich cycles from the Kimmeridge Clay Formation of Yorkshire (G.B.): productivity vs. anoxia. *Palaeogeogr. Palaeoclimatol. Palaeoecol.* 108, 165–181.
- Tribouvillard, N., Bialkowski, A., Tyson, R.V., Vergès, E., Deconinck, J.-F., 2001. Organic facies and sea level variation in the Late Kimmeridgian of the Boulonnais area northernmost France). *Mar. Petrol. Geol.* 18, 371–389.
- Tribouvillard, N., Trentesaux, A., Ramdani, A., Baudin, F., Riboulleau, A., 2004a. Contrôles de l'accumulation de matière organique dans la Kimmeridge Clay Formation (Jurassique supérieur, Yorkshire, G.B.) et son équivalent latéral du Boulonnais: l'apport des éléments traces métalliques. *Bull. Soc. Géol. Fr.* 175, 491–506.
- Tribouvillard, N., Riboulleau, A., Lyons, T., Baudin, F., 2004b. Enhanced trapping of molybdenum by sulfurized organic matter of marine origin as recorded by various Mesozoic formations. *Chem. Geol.* 213, 385–401.
- Tribouvillard, N., Ramdani, A., Trentesaux, A., 2005. Controls on organic accumulation in Late Jurassic shales of Northwestern Europe as inferred from trace-metal geochemistry. In: Harris, N. (Ed.), *The Deposition of Organic-Carbon-Rich Sediments: Models, Mechanisms, and Consequences*. SEPM Spec. Public., 82, pp. 145–164.
- Tribouvillard, N., Algeo, T., Lyons, T.W., Riboulleau, A., 2006. Trace metals as paleoredox and paleoproductivity proxies: an update. *Chem. Geol.* 232, 12–32.
- Tribouvillard, N., Lyons, T.W., Riboulleau, A., Bout-Roumazielles, B., 2008. A possible capture of molybdenum during early diagenesis of dysoxic sediments. *Bull. Soc. Geol. Fr.* 179, 3–12.
- Tyson, R.V., 1995. *Sedimentary organic matter: organic facies and palynofacies*. Chapman & Hall, London. 615 p.
- Tyson, R.V., Follows, B., 2000. Palynofacies prediction of distance from sediment source: a case study from the Upper Cretaceous of the Pyrenees. *Geology* 28, 569–571.
- Van Cappellen, P., Viollier, E., Roychoudhury, A., Clark, L., Ingall, E., Lowe, K., DiChristina, T., 1998. Biogeochemical cycles of manganese and iron at the oxic-anoxic transition of a stratified marine basin (Orca Basin, Gulf of Mexico). *Environ. Sci. Technol.* 32, 2931–2939.
- Van der Weijden, C.H., 2002. Pitfalls of normalization of marine geochemical data using a common divisor. *Mar. Geol.* 184, 167–187.
- Vorlicek, T.P., Helz, G.R., 2002. Catalysis by mineral surfaces: implications for Mo geochemistry in anoxic environments. *Geochim. Cosmochim. Acta* 66, 3679–3692.
- Vorlicek, T.P., Kahn, M.D., Kasuza, Y., Helz, G.R., 2004. Capture of molybdenum in pyrite-forming sediments: role of ligand-induced reduction by polysulfides. *Geochim. Cosmochim. Acta* 68, 547–556.
- Weber, F.F., Sackett, W.M., 1981. Uranium geochemistry of Orca Basin. *Geochim. Cosmochim. Acta* 45, 1321–1329.
- Wedepohl, K.H., 1971. Environmental influences on the chemical composition of shales and clays. In: Ahrens, L.H., Press, F., Runcorn, S.K., Urey, H.C. (Eds.), *Physics and Chemistry of the Earth*. Pergamon, Oxford, pp. 305–333.
- Wedepohl, K.H., 1991. The composition of the upper Earth's crust and the natural cycles of selected metals. In: Merian, E. (Ed.), *Metals and Their Compounds in the Environment*. VCH-Verlagsgesellschaft, Weinheim, pp. 3–17.
- Wiesenburg, D.A., Brooks, J.M., Bernard, B.B., 1985. Biogenic hydrocarbon gases and sulfate reduction in the Orca Basin brine. *Geochim. Cosmochim. Acta* 49, 2069–2080.
- Wong, G.T.F., Takayanagi, K., Todd, J.F., 1985. Dissolved iodine in waters overlying and in the Orca Basin, Gulf of Mexico. *Mar. Chem.* 17, 177–183.
- Zheng, Y., Anderson, R.F., van Geen, A., Kuwabara, J., 2000. Authigenic molybdenum formation in marine sediments: a link to pore water sulfide in the Santa Barbara Basin. *Geochim. Cosmochim. Acta* 64, 4165–4178.